Self Organized Criticality in Digging Myopic Ant Model.

Prashant M. Gade[1*] and M. P. Joy[2†]

[1] *Jawaharlal Nehru Centre for Advanced Scientific Research, Jakkur, Bangalore-560064, INDIA*

[2] *Materials Research Centre, Indian Institute of Science, Bangalore-560012, INDIA*

Abstract

We demonstrate the phenomenon of self organized criticality (SOC) in a simple random walk model described by a random walk of a myopic ant. The ant acts on the underlying lattice aiming at uniform digging of the surface but is unaffected by the underlying lattice. In 1-d, 2-d and 3-d we have explored this model and have obtained power laws in the time intervals between consecutive events of 'digging'. Being a simple random walk, the power laws in space translate to power laws in time. We also study the finite size scaling of asymptotic scale invariant process as well as dynamic scaling in this system. This model differs qualitatively from the cascade models of SOC.

PACS Nos : 05.40.+j; 68.35.Fx; 47.55.Mh.

The concept of self organized criticality (SOC) was introduced by Bak, Tang and Wiesenfeld in the context of avalanches in sandpile model (BTW model) [1]. Diffusively coupled spatially extended system which is driven adiabatically, i.e. the drive occurs only when system has been fully relaxed, settles in the metastable state with very long correlations and no characteristic length scale. This model is termed to be self organized since the critical state is reached, though no particular parameter seems to have been adjusted. There have been further variants of the above model which have similar rules, but are in different universality class [2]. The above models are cellular automata models in which the discrete variable value assigned to different points on a d-dimensional lattice are updated in discrete time [3]. The relevant perturbations in which SOC gets destroyed has been a topic of interest to many researchers [4]. Developing a PDE model for SOC has also been an active area of interest [5]. There have been models with threshold dynamics in continuous variable values like adaptive dynamics model on coupled map lattices or earthquake models, though it is debatable whether the power laws arising in these models can be termed as self organized [6,7].

In all these models SOC is induced by a branching process. The disturbance propagates from one length scale to the other by branching in various directions and this hierarchical basis for the dynamics leads to a power-law behavior. This description of branching leading to power laws has been given for as diverse processes as intermittent turbulent process by Kolmogorov [8] or income distributions in US by Schlesinger [9]. However, scale invariant processes need not be produced by branching alone. The disturbance can choose a random direction yielding scale invariant structure. Here we propose a simple random walk model for SOC. As a physical illustration, we would like to note a recent experimental observation by Vishwanathan *et al* [10] about foraging behavior of sea-birds. In this experiment, the authors studied the foraging behavior of wandering albatross. Measurements of the distance travelled by the bird at various times are carried out. They found a power law behavior in distribution of flight time events. Interestingly, the observation is that though the distribution deviates significantly from simple random walk, it is still a power law implying a scale invariant

manner in which the flights proceed. Assuming that the flight directions change randomly after finding food, they argued that the data they have suggests that the distribution of food on the ocean surface is also scale invariant. Although we do not attempt to model this experiment, it nicely illustrates the fact that not only the branching processes but the processes induced by simple random walk/flight also can organize themselves in a scale invariant fashion in time and space.

We introduce a new model of self organized scale invariant behavior in space and time which is induced by random walk. A model of Eulerian walkers(EW) has been introduced recently [11]. Our model is simpler in the sense that unlike the above model, the walker is unaffected by the medium. As it will be clear in the course of discussion, not only it is in a different universality class, but is even qualitatively different from the earlier models.

Let us first discuss our model in 1-dimension for simplicity. We consider a lattice of length L. At each site i, $1 \leq i \leq L$, we associate an integer, x_i which denotes the height of that point and $-\infty < x_i \leq 0$. To begin with, we assign $x_i = 0$ for all i. We put a random walker at a randomly chosen site j, $(1 \leq j \leq L)$. Now the dynamics of the lattice is defined in the following way. (a) At each time step, the random walker moves to its nearest neighbor which is chosen randomly. (b) Before moving to the next site, the random walker compares the height at that site with those of nearest neighbors and reduces the height at that site by 1 unless any of the nearest neighbors has a higher height. In other words, if random walker is at site k, then

$$x_k = x_k - 1 \;\text{ unless }\; x_{k+1} > x_k \text{ or } x_{k-1} > x_k.$$

We will note this event of reduction of height as 'digging'. The condition above on digging is introduced since the aim of the random walker is to dig uniformly and it does not want to dig the site which already has a height lower than any of its neighbors. Though the medium is affected by the walk, the walker is unaffected by the medium, i.e. the next site to which the random walker moves is chosen randomly and is independent of the entire height profile. At boundaries the comparison is only one sided. If the random walker

moves out of the lattice, we put it back in a randomly chosen site within the lattice. Since the random walker can not see beyond nearest neighbors we call the model as digging myopic ant (DMA) model. We can also describe the model in terms of the evolution rule for the slopes on either side of the random walker. (By construction the slopes can take only three values 1,0, and -1.) Of the nine possible combination, four of them transform as $1, 0 \longrightarrow 0, 1$; $1, -1 \longrightarrow 0, 0$; $0, 0 \longrightarrow -1, 1$; $0, -1 \longrightarrow -1, 0$ while the rest five remain unchanged. (See Fig. 1.) The rule at the left boundary is $0 \longrightarrow 1$; $-1 \longrightarrow 0$ and $1 \longrightarrow 1$ while at the right boundary $1 \to 0$, $0 \to -1$ and $-1 \to -1$. Note that except at boundaries the sum of slopes remains conserved.

We start with a flat surface. This means that in the beginning all sites are potentially 'active', i.e. can be dug. However, as the surface evolves, all kinds of valleys appear in the interface and only a few sites at the top of the valley remain active. If one ignores the fact that the sites dug subsequently are not independent of each other, rather are spatially nearby, i.e. the noise in our case is correlated, one can relate the distribution of times required to reach active sites to the spatial distribution of active sites. Now we look at the distribution of time intervals between which active sites were visited.

Here, the system is driven by random perturbations and the time interval t between two successive events of digging when the medium is affected by the walker is a quantity of interest. We compute the distribution $P(t)$ where $P(t)$ is the normalized probability that the time between two successive events of digging is t. We also compute the probability distribution $D(s)$, the number of distinct sites s visited by the random walker between two successive events. We find that $P(t) \sim t^{-\gamma}$, $\gamma \approx 1.6$. It is clear that the distribution $D(s)$ can not be independent of $P(t)$ since in a simple random walk number of distinct sites s visited in time t goes as $t^{\frac{1}{2}}$. This implies $D(s) \sim s^{-\gamma'}$, $\gamma' = 2\gamma - 1$. Thus as one would expect, a power law distribution in time translates in a power law distribution in space. Fig. 2(a) and Fig. 2(b) show $P(t)$ and $D(s)$ for various lattice sizes in 1-d. If one looks at the spatial profile of the lattice developed after a long time, one can see valleys of all sizes. Thus a myopic random walker who started the walk aiming at a uniform digging of the surface,

ends up digging the surface in a scale invariant manner. Thus unlike BTW model, this model shows nontrivial nontransient scaling properties even in one dimension. However, we note that it has properties common with earlier SOC models. It is a conservative model except at the boundaries in the sense that the sum of slopes at all the sites does not change unless digging occurs at the boundary. As in earlier model, the boundary conditions are open. However, as seen above, evolution rule described in terms of local slopes is anisotropic. The relation with the distribution of active sites is not clear since noise is correlated.

Given the nature of the distributions, i.e. a simple power law followed by an exponential tail, one can fit a finite size scaling form $P(t,L) = L^{\mu}G(t/L^{\nu}), D(s,L) = L^{\mu'}F(s/L^{\nu'})$, ($\mu = \gamma\nu$ and $\mu' = \gamma'\nu'$), to the distributions [12]. In 1-d we can fit the scaling nicely with $\nu = 2, \nu' = 1$. This is useful in higher dimensions in particular where it is difficult to do a very large size simulations and scaling form gives the power law exponents with reasonable accuracy. In the Fig. 2 depicting the distributions $P(t)$ and $D(s)$, we also show the finite-size scaling in the inset.

The model can be easily extended to higher dimensions. We have studied this model in two and three dimensions. We plot inter-event time distribution $P(t)$ in 2-d and 3-d in Fig. 3(a) and Fig. 4. As in 1-d, $P(t) \sim t^{-\gamma}$ with $\gamma \approx 1.2, \nu \approx 2$ in 2-d and $\gamma \approx 1.2, \nu \approx 1.8$ in 3-d. Since the number of distinct sites covered s goes as $t/ln(t)$ in 2-d and as t in 3-d [13], one can expect a power law distribution for $D(s)$ as well with $\gamma' = \gamma$ except that one expects a logarithmic correction in 2-d (which was not possible to detect for the sizes to which we could carry out the simulations). Fig. 3(b) shows the distribution $D(s)$ in 2-d. For 3-d, site distribution was beyond our available computational resources. However, we expect it to closely follow the $P(t)$. In Figures 3 and 4, the insets show the finite size scaling in each of the cases as in Fig. 2. The geometrical picture in 2-d is identical to that in 1-d. One sees valleys of all sizes present in the asymptotic height profile in 2-d. This is understandable. Like in sandpile model if one has a configuration with a single big valley, the random walker can go to the boundary and dig making sites in the interior active and thus one expects many events. (In our model, one more configuration in which not many

sites will be active will be a long tilted interface. However, by the same logic, it will not stay for long.) Similarly, starting with a flat interface, one expects many events since all sites are active. Thus the surviving configuration, or the configuration which will be attained most of times will be the one in which valleys of all sizes are present.

We have also seen how the profile changes in time. The simplest quantitative measure that demonstrates the geometrical changes in the profile is roughness. The roughness $\sigma(L,t)$ of the interface of length L at time t (starting with a flat interface) is given by $\sigma(t,L) = \sqrt{\frac{1}{L}\sum_{i=1}^{L}(x_i(t) - \bar{x}(t))^2}$, where $\bar{x}(t)$ is the average height of the interface at time t. Growth depends on nearest neighbors and thus the correlations develop in time and span the entire length L. When the entire surface gets correlated the width saturates. The roughness $\sigma(L,t)$ follows a scaling relation, $\sigma(t,L) = L^{\alpha} f(t/L^{z})$ (See *e.g.* [14]). The exponent $z = \alpha/\beta + 1$. The exponent $\beta = 0.565$ signifies the growth in time in the begining ($\sigma(t,L) \sim t^{\beta}$), z gives saturation time ($t_{sat} \sim L^{z}$) and $\alpha = 1.1$ signifies saturation width ($\sigma_{sat} \sim L^{\alpha}$). The scaling form with the above fit which assumes a power-law growth followed by saturation is reasonably good (see Fig. 5). For small times ($t < 9,\ L >> t$) one can easily compute all the possible configurations and their probabilities analytically. The values computed so are in close agreement with simulations and also yield the growth exponent $\beta = 0.565$. Large value of α reflects the highly inhomogeneous asymptotic interface.

We have also studied a variant of the model in which one tries to reduce the correlation between successive events by putting the random walker in a random position after each digging. Thus the noise is not spatially correlated any longer. Most of the qualitative features of the model do not change. The dynamic scaling in this variant and further investigations in the current model as well as its variant are deferred to a future publication.

In short, we have proposed a new model of self organized criticality in which the governing mechanism is that of diffusion. This model is hopefully easier to handle analytically since the exponents in space are easily related to exponents in time and one does not have a lot of unrelated and and ill-understood exponents. We also feel that such models could be of use in situations which yield scale invariant behavior but do not involve cascades, but rather

have diffusion as the only way in which information spreads in the system.

Authors have enjoyed discussions with N. Kumar and G. Ananthakrishna. PMG acknowledges correspondence with D. Dhar. MPJ acknowledges financial support from IFC-PAR Grant no.1108-1.

REFERENCES

* email : prasha@jnc.iisc.ernet.in

† email : joy@mrc.iisc.ernet.in

[1] P. Bak, C. Tang and K. Wiesenfeld, Phys. Rev. Lett. **59**, 381 (1987).

[2] S. S. Manna, L. B. Kiss and J. Kertész, J. Stat. Phys. **22**, 923 (1990).

[3] For a similar model with continuous values of local variables see Y.-C. Zhang, Phys. Rev. Lett. **63**, 470 (1989).

[4] See for example, B. Tadic and R. Ramaswamy, Phys. Rev. E **54**, 3157 (1996).

[5] G. Grinstein, D.-H. Lee and S. Sachdev, Phys. Rev. Lett. **64**, 1927 (1990); L. Gil and D. Sornette, Phys. Rev. Lett. **76**, 3991 (1996).

[6] S. Sinha and D. Biswas, Phys. Rev. Lett. **71**, 2010 (1993).

[7] J. M. Carlson and J. S. Langer, Phys. Rev. Lett. **62**, 2632 (1989); Phys. Rev. A **40**, 6470 (1989).

[8] See for example, T. E. Faber, *Fluid Dynamics for Physicists*, (Cambridge University Press, Cambridge, 1995).

[9] M. F. Schlesinger, in *Growth and Form*, edited by H. E. Stanley, and N. Ostrowski, (Nijhoff, Dordecht, 1986), p. 283.

[10] G. M. Vishwanathan *et al* Nature **381**, 413 (1996).

[11] V. B. Priezzhev, D. Dhar, A. Dhar and S. Krishnamurthy, Phys. Rev. Lett. **77**, 5079 (1996).

[12] L. P. Kadanoff *et al*, Phys. Rev. A **39**, 6524 (1989).

[13] See *e.g.*A. M. Nemirovsky, H. O. Martin and M. D. Coutinho-Filho, Phys. Rev. A **41**, 761 (1990).

[14] A. -L. Barabási and H. E. Stanley, *Fractal Concepts in Surface Growth*, (Cambridge University Press, Cambridge, 1995).

FIGURES

FIG. 1. Schematic diagram of the configurations that change by the action of the random walker which is at the centre. Slopes are also shown.

FIG. 2. (a)The inter-event time distribution, $P(t, L)$ *vs* time t in 1-d. (b)Probability distribution $D(s, L)$ that s distinct sites are visited between two events, *vs* s in 1-d. (In both figures $A)\, L = 10$, $B)\, L = 25$, $C)\, L = 50$, $D)\, L = 100$ and $E)\, L = 1000$. Insets show finite size scaling.)

FIG. 3. (a)$P(t, L)$ *vs* time t in 2-d. (b)$D(s, L)$ *vs* s in 2-d. (In both figures $A)\, L = 10$, $B)\, L = 25$, $C)\, L = 50$, $D)\, L = 100$ and $E)\, L = 200$. Insets show finite size scaling.)

FIG. 4. $P(t, L)$ *vs* t in 3-d. Inset shows finite size scaling.

FIG. 5. Roughness $\sigma(t, L)$ *vs* time t for various L in 1-d. Inset shows the dynamic scaling of the interface.

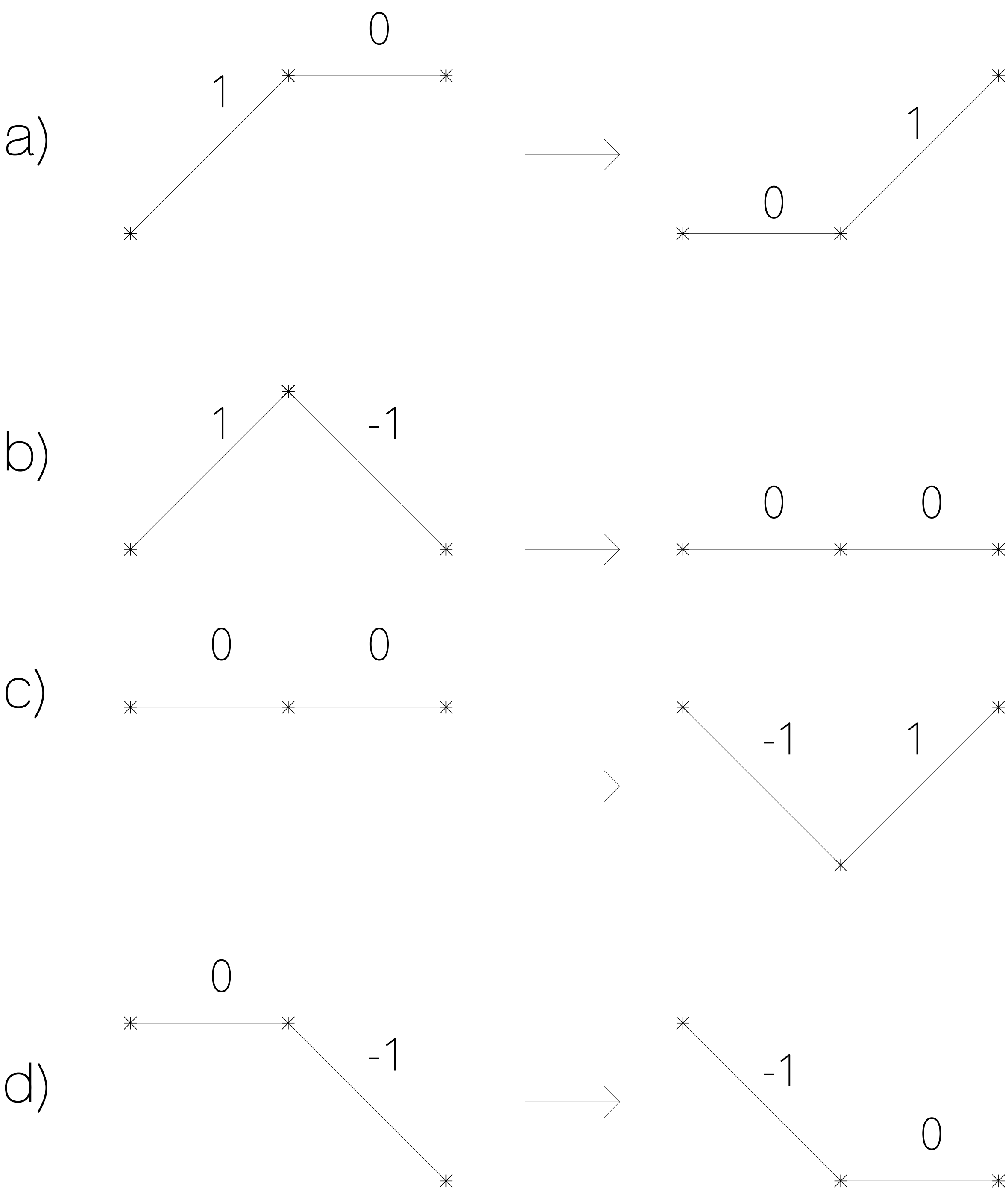
a)
1
0
0
1
b)
1
-1
0
0
c)
0
0
-1
1
d)
0
-1
-1
0

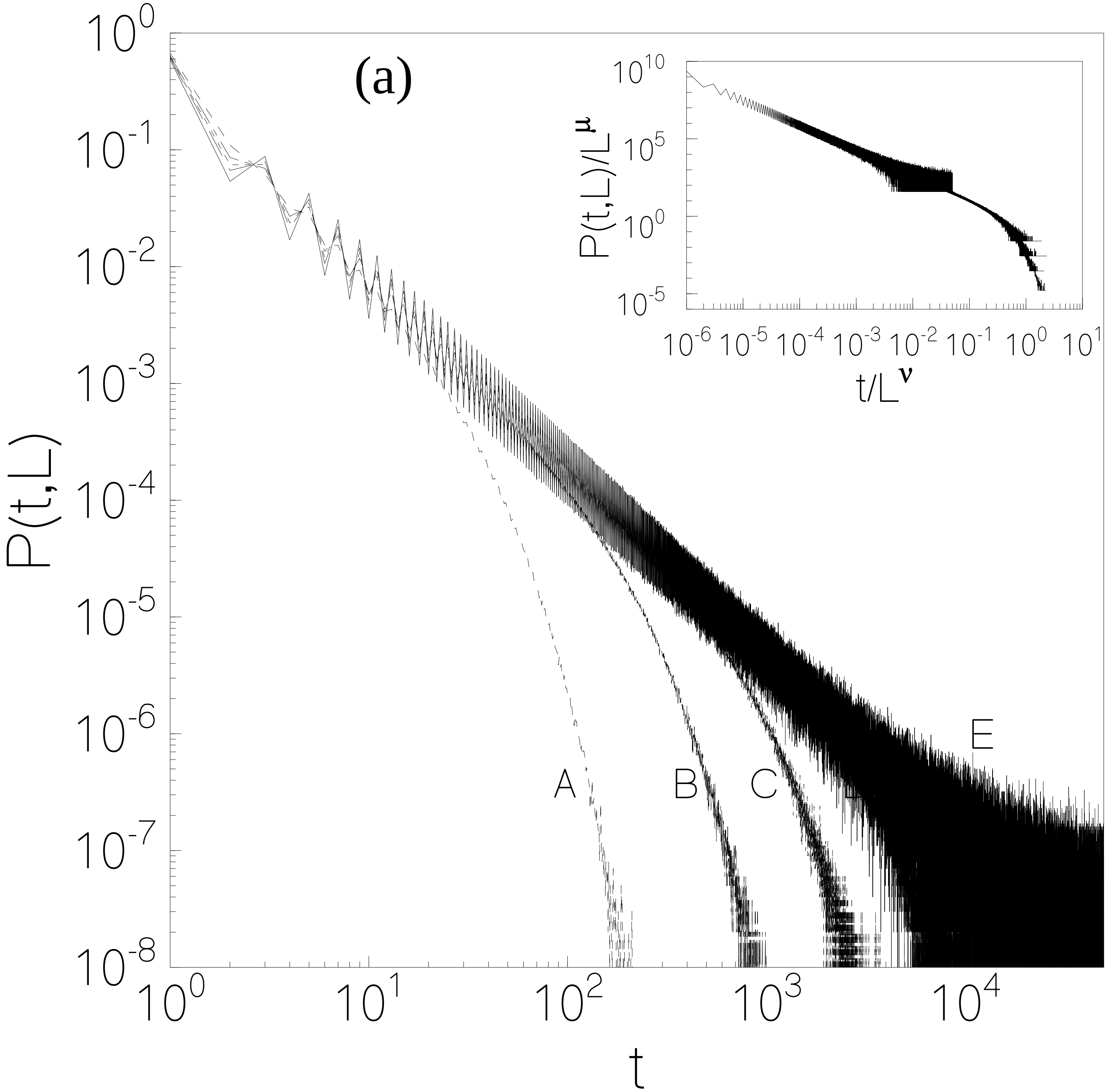

(a)
P(t,L)
t
A
B
C
E
P(t,L)/L^μ
t/L^ν

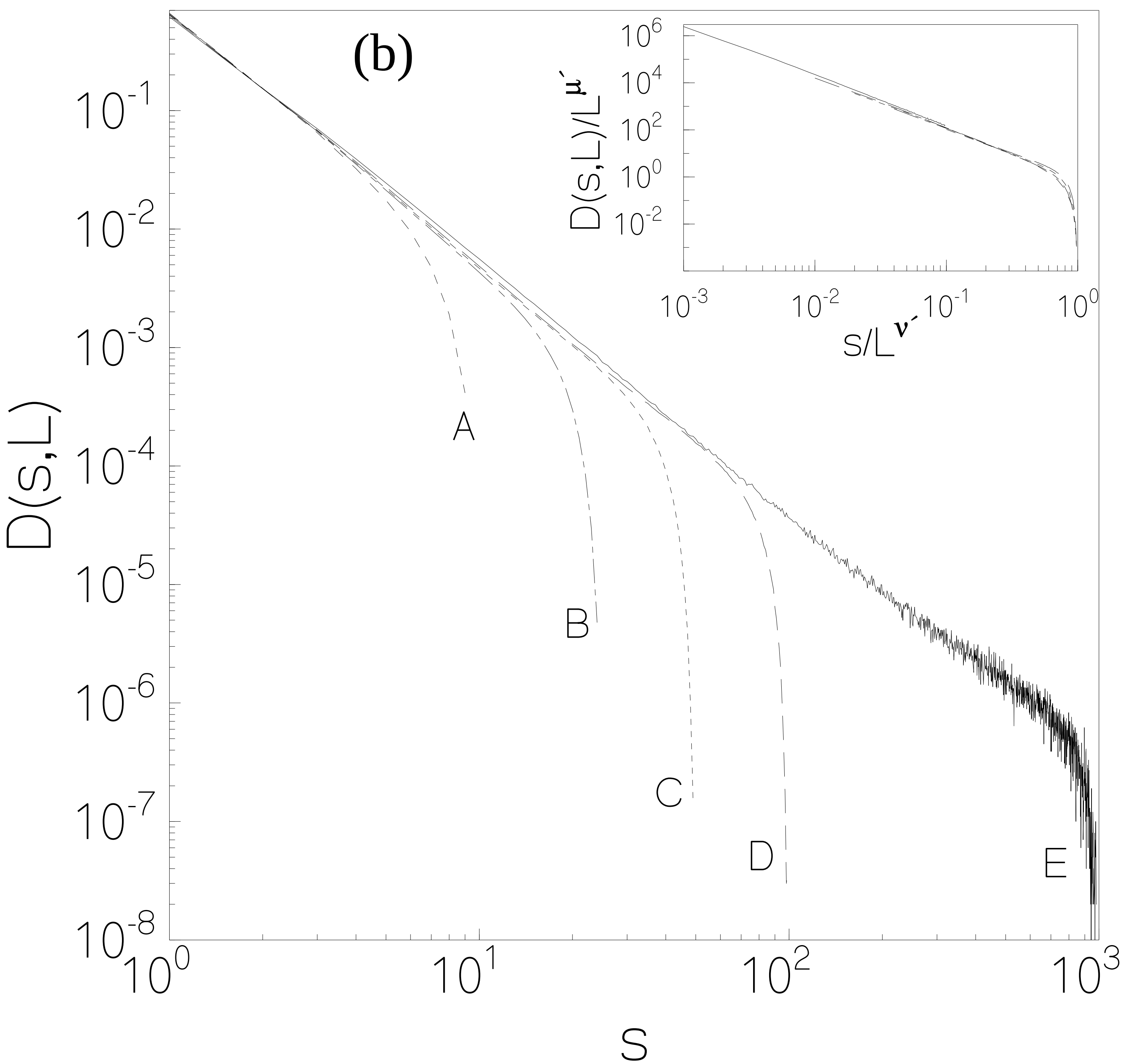

(b)
D(s,L)
s
A
B
C
D
E
10^-8
10^-7
10^-6
10^-5
10^-4
10^-3
10^-2
10^-1
10^0
10^1
10^2
10^3
D(s,L)/L^μ´
s/L^ν´
10^6
10^4
10^2
10^0
10^-2
10^-3
10^-2
10^-1
10^0

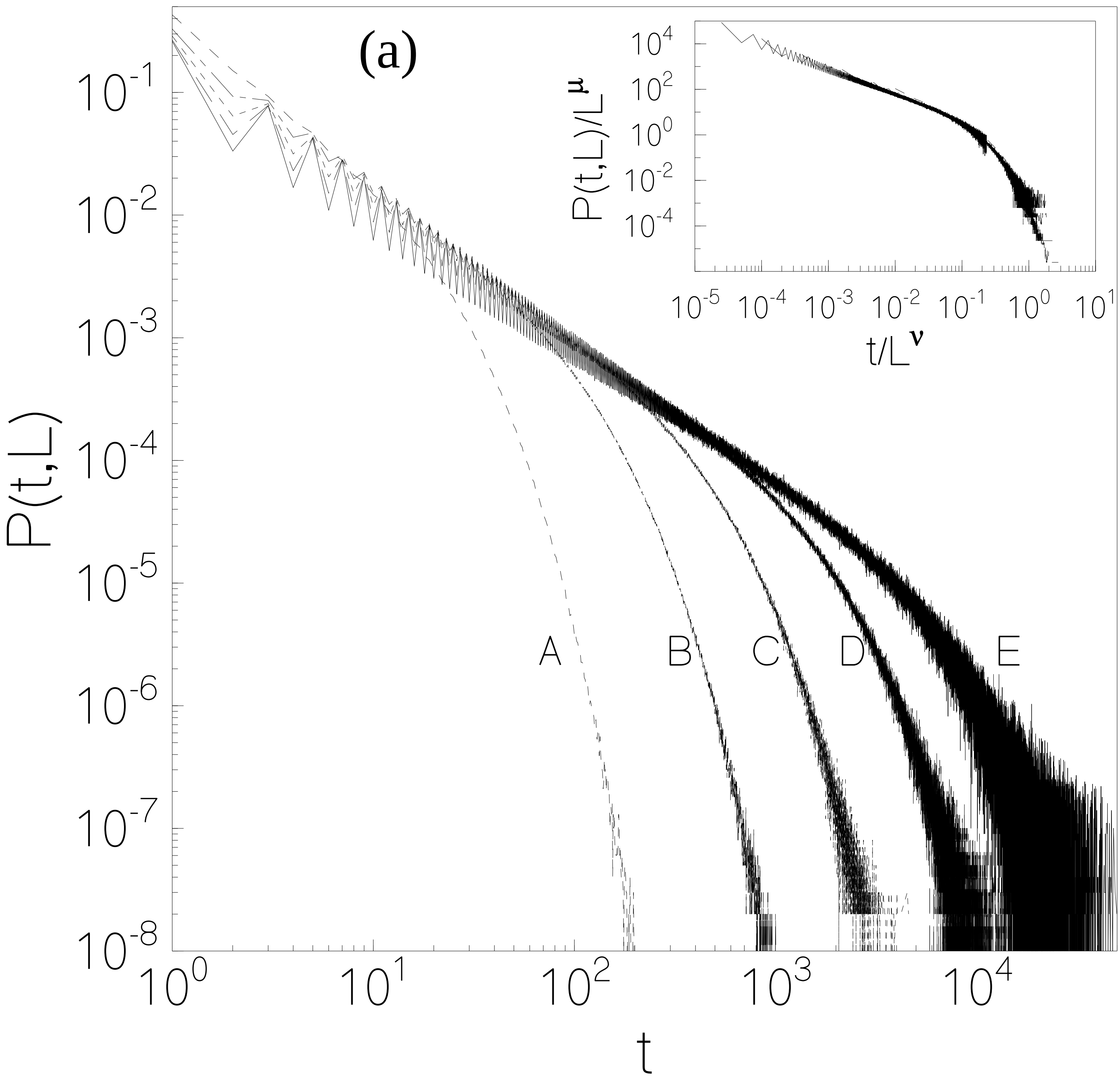

(a)
P(t,L)
t
A
B
C
D
E
P(t,L)/L^μ
t/L^ν

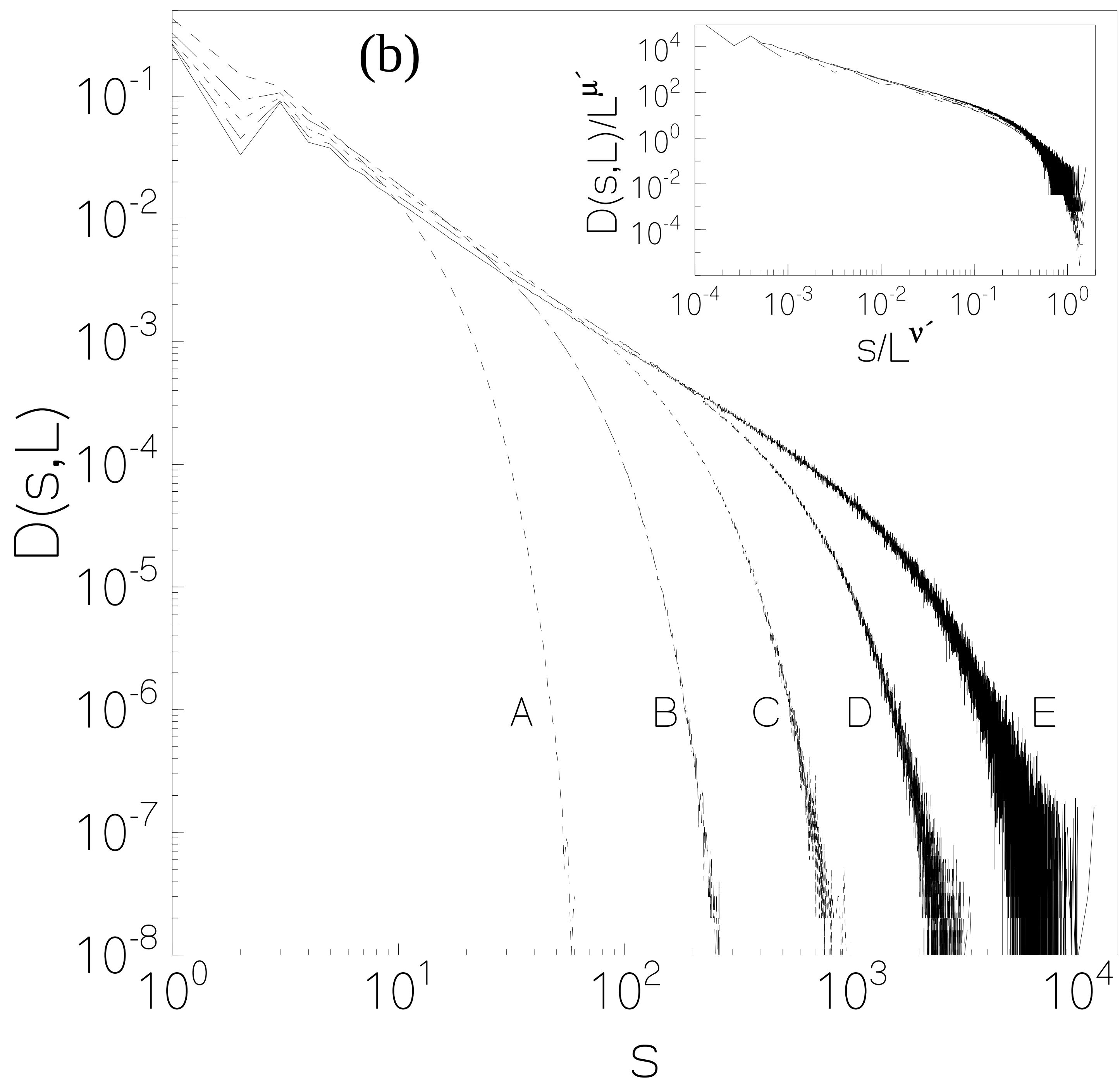

(b)
D(s,L)
s
A
B
C
D
E
D(s,L)/L^μ´
s/L^ν´

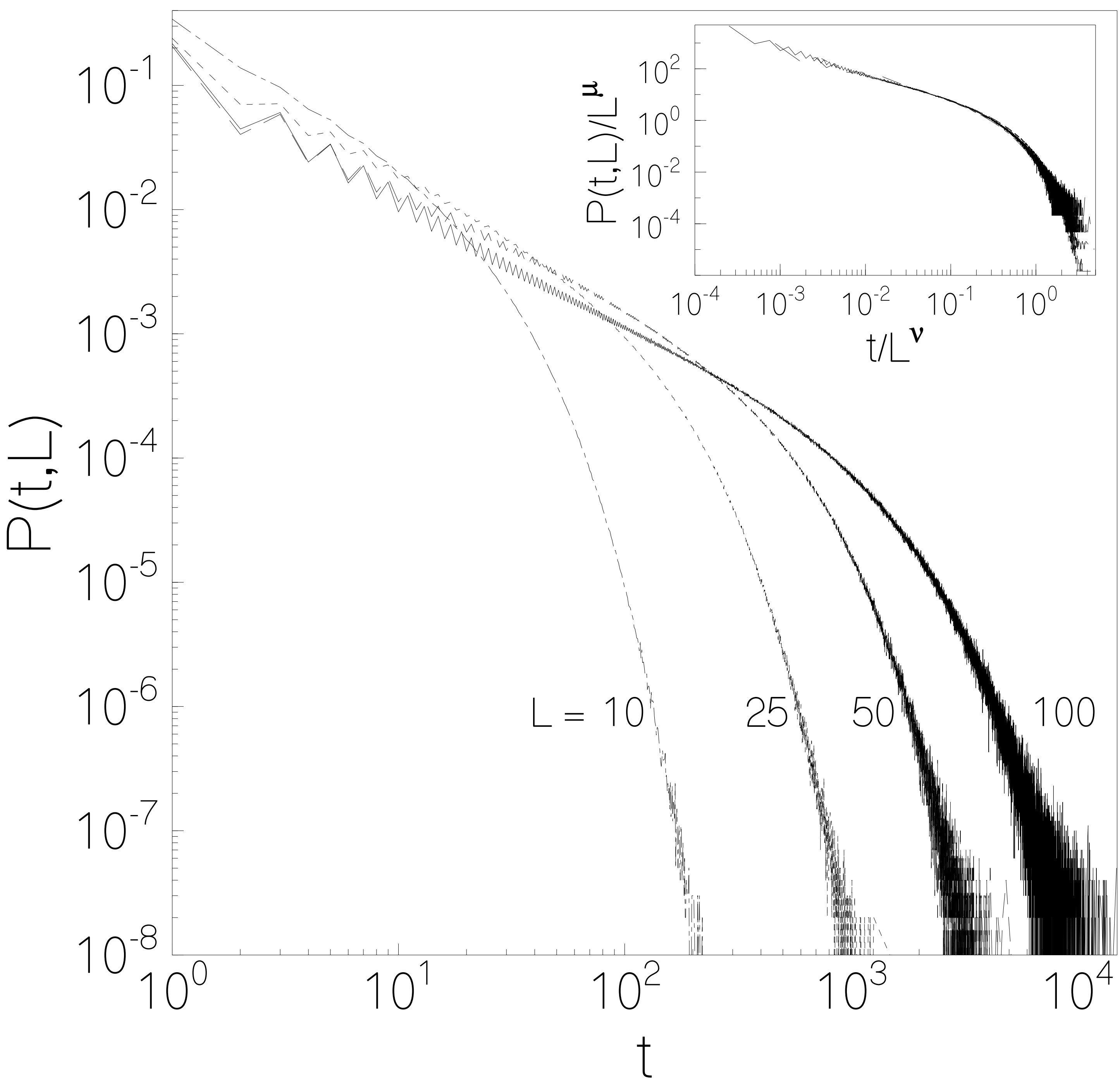

P(t,L)
t
L = 10
25
50
100
P(t,L)/L^μ
t/L^ν

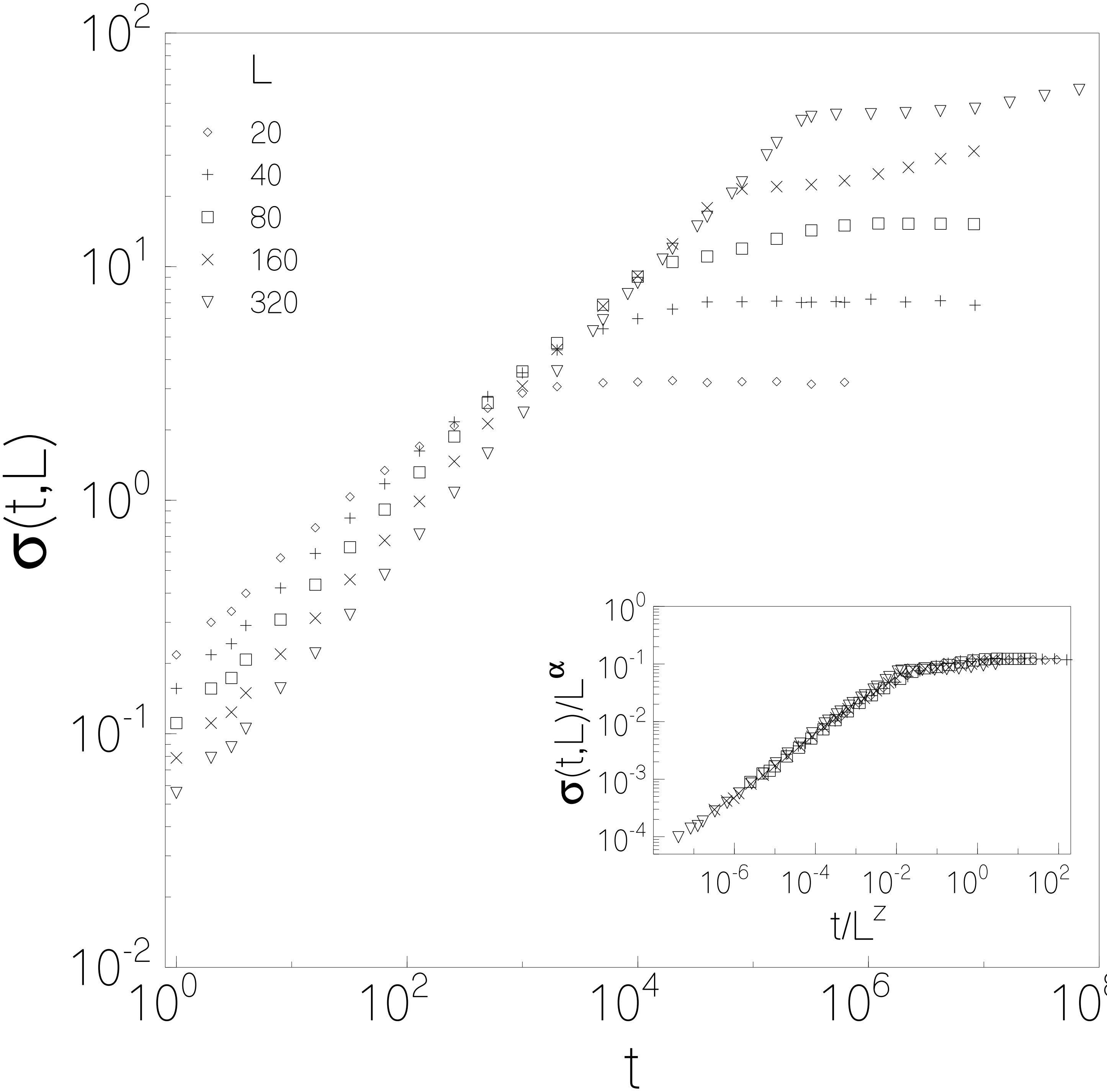

$\sigma(t,L)$
t
L
20
40
80
160
320
10^{-2}
10^{-1}
10^{0}
10^{1}
10^{2}
10^{0}
10^{2}
10^{4}
10^{6}
10^{8}
$\sigma(t,L)/L^{\alpha}$
t/L^{z}
10^{-4}
10^{-3}
10^{-2}
10^{-1}
10^{0}
10^{-6}
10^{-4}
10^{-2}
10^{0}
10^{2}